Neuropharmacology 56 (2009) 665–675

Contents lists available at ScienceDirect

Neuropharmacology

journal homepage: www.elsevier.com/locate/neuropharm

Calcium channel dysfunction in inferior colliculus neurons of the genetically epilepsy-prone rat

Prosper N'Gouemo [a,*], Carl L. Faingold [b], Martin Morad [c,1]

[a] Department of Pediatrics, Georgetown University Medical Center, 3900 Reservoir Rd, NW, Washington, DC 20057, United States
[b] Department of Pharmacology, Southern Illinois University School of Medicine, P.O. Box 19629, Springfield, IL 62794, United States
[c] Department of Pharmacology, Georgetown University Medical Center, 3900 Reservoir Rd, NW, Washington, DC 20057, United States

ARTICLE INFO

Article history:
Received 31 March 2008
Received in revised form
25 November 2008
Accepted 26 November 2008

Keywords:
Ca^{2+} channel current
L-type
N-type
R-type
Reflex audiogenic seizure

ABSTRACT

Voltage-gated calcium (Ca^{2+}) channels are thought to play an important role in epileptogenesis and seizure generation. Here, using the whole cell configuration of patch-clamp techniques, we report on the modifications of biophysical and pharmacological properties of high threshold voltage-activated Ca^{2+} channel currents in inferior colliculus (IC) neurons of the genetically epilepsy-prone rats (GEPR-3s). Ca^{2+} channel currents were measured by depolarizing pulses from a holding potential of −80 mV using barium (Ba^{2+}) as the charge carrier. We found that the current density of high threshold voltage-activated Ca^{2+} channels was significantly larger in IC neurons of seizure-naive GEPR-3s compared to control Sprague–Dawley rats, and that seizure episodes further enhanced the current density in the GEPR-3s. The increased current density was reflected by both a −20 mV shifts in channel activation and a 25% increase in the non-inactivating fraction of channels in seizure-naive GEPR-3s. Such changes were reduced by seizure episodes in the GEPR-3s. Pharmacological analysis of the current density suggests that upregulation of L-, N- and R-type of Ca^{2+} channels may contribute to IC neuronal hyperexcitability that leads to seizure susceptibility in the GEPR-3s.

1. Introduction

Epilepsies are disorders of neuronal excitability and considerable evidence suggests that aberrances in calcium (Ca^{2+}) channel currents contribute to epileptogenesis and seizure generation. For instance, mutations in genes encoding the Ca^{2+} channel α1A, β4 and α2δ subunits predispose mice to generalized seizures (Fletcher et al., 1996; Burgess et al., 1997). Similarly, Ca^{2+} channel mutations also may be responsible for the juvenile myoclonic and idiopathic generalized epilepsies in the human (Escayg et al., 2000; Chioza et al., 2001; Jouvenceau et al., 2001). Animal models of epilepsy with inherited susceptibility to seizures provide unique opportunities to study the cellular and molecular mechanisms underlying chronic neuronal hyperexcitability that leads to seizures (Stables et al., 2002). The genetically epilepsy-prone rat (GEPR) is a well-validated animal model for generalized tonic/clonic epilepsy in the human (Faingold, 1999; Jobe and Browning, 2006). In this model, generalized clonic/tonic seizures are triggered by exposure to auditory stimuli; these seizures are referred to as reflex audiogenic seizures. Two separate substrains of the GEPRs (3 and 9) have been identified based on the seizure phenotype, with the GEPR-9s exhibiting generalized tonic seizures, and GEPR-3s displaying generalized clonic seizures. Multiple lines of evidence indicates that the inferior colliculus (IC) is the primary site for the initiation of these reflex audiogenic seizures in the GEPRs (Browning, 1986; Faingold, 1999). Electrophysiological studies suggested that neurons in the IC, unlike in other brain areas, exhibited a sustained increase in neuronal firing during the transition to seizures; this chronic neuronal hyperexcitability is thought to be critical for seizure initiation in the GEPR-9s (N'Gouemo and Faingold, 1996, 1998; Faingold, 1999; Fen and Faingold, 2002; Raisinghani and Faingold, 2005a,b). Such changes in IC neuronal firing also may occur in the GEPR-3s. In the GEPRs, the mechanisms underlying chronic IC neuronal hyperexcitability that leads to seizure susceptibility are not yet fully understood (Faingold et al., 1986; Evans et al., 1994; Li et al., 1994; Verma-Ahuja et al., 1995; N'Gouemo and Faingold, 1996; Dailey et al., 2001).

In an animal model for alcohol withdrawal the IC similarly appears to be a critical component of the neuronal networks for reflex audiogenic seizures (Frye et al., 1983; Chakravarty and Faingold, 1998; Faingold et al., 1998, 2004; N'Gouemo and Rogawaski, 2006). We have recently shown that the current density of high threshold voltage-activated (HVA) Ca^{2+} channels was significantly increased in IC neurons of rats exhibiting enhanced

* Corresponding author. Tel.: +1 202 687 8464; fax: +1 202 687 8458.
E-mail address: pn@georgetown.edu (P. N'Gouemo).
[1] Present address: Department of Cell Biology and Anatomy, University of South Carolina School of Medicine, Columbia, SC 29208, United States.

0028-3908/$ – see front matter © 2008 Elsevier Ltd. All rights reserved.
doi:10.1016/j.neuropharm.2008.11.005

susceptibility to reflex audiogenic seizures following alcohol withdrawal (N'Gouemo and Morad, 2003a). Consistent with this observation, Ca^{2+} channel antagonists have been reported to suppress reflex audiogenic seizures in rats subjected to alcohol withdrawal as well as in the GEPR-3s and GEPR-9s providing a causal relation between Ca^{2+} channels and audiogenic seizure susceptibility (Little et al., 1986; De Sarro et al., 1990). Whether Ca^{2+} channel current density in IC neurons of the GEPR-3s is similarly enhanced as in rats subjected to alcohol withdrawal remains unknown. Accordingly, we examined the biophysical and pharmacological properties of HVA Ca^{2+} channels in IC neurons of the GEPR-3s. Here, we report that seizure susceptibility alters the gating properties of Ca^{2+} channels and increases the expression of select types of HVA Ca^{2+} channel currents in IC neurons of the GEPR-3s. A preliminary report of this study has already appeared (N'Gouemo et al., 2004).

2. Methods

2.1. Animals

Male GEPR-3s (8–12 week-old) were obtained from the colonies maintained at Southern Illinois University, Springfield, IL and at Georgetown University, Washington, DC. This animal strain was derived from Sprague–Dawley (SD) rats by selective breeding for audiogenic seizure susceptibility (Jobe and Laird, 1981). Age-matched SD rats purchased from Taconic (Germantown, NY) were used as controls. The animals were placed in plastic cages with free access to food and water, and housed in a loud sound-restricted environment (20–60 db SPL) with controlled temperature and humidity, as well as a standard day/night cycle. Spontaneous seizures are rare in the GEPR-3s and were not monitored in this study. Two groups of GEPR-3 were used. The seizure-naive GEPR-3s (SN-GEPR-3s) refer to animals that have never been exposed to sound stimulus-induced seizures, while seizure experienced GEPR-3s (SE-GEPR-3s) refer to animals that have been exposed to loud sound stimulus-induced seizures and that have exhibited generalized seizures corresponding to score 3 on the scale of reflex audiogenic seizures (Jobe et al., 1973; Reigel et al., 1986). Seizure-naive GEPR-3s and SE-GEPR-3s were selected randomly from the colonies. In order to elicit reflex audiogenic seizures, GEPR-3s were exposed to an electrical bell (120 dB SPL, re: 0.0002 dynes/cm^2) until seizure onset or for a maximum of 60 s. In this study, all SE-GEPR-3s exhibited one episode of reflex audiogenic seizures consisting of wild running that evolves into generalized clonic seizures. Seizure-experienced GEPR-3s were used 4–6 weeks after seizure induction for electrophysiological studies; this time interval avoids the effects of acoustic stimulation and acute effects of seizures themselves on voltage-gated Ca^{2+} channel currents. All experimental procedures were approved by the Institution Animal Care and Use Committee, and all efforts were made to minimize the number of animals used and their suffering.

2.2. Cell preparation

Dissociated IC neurons were obtained as previously described (N'Gouemo and Morad, 2003a,b). Briefly, rats were anesthetized with pentobarbital (50 mg/kg, i.p.). The brains were perfused with a solution containing (in mM): 110 choline chloride, 2.5 KCl, 1.2 NaH_2PO_4, 26 $NaHCO_3$, 2.4 sodium/pyruvate, 1.3 L-ascorbic acid, 20 dextrose, 0.5 $CaCl_2$ and 7 $MgCl_2$ (290–300 mOsm with sucrose, bubbled with 95% O_2 and 5% CO_2). Brains were removed and immersed in sucrose solution containing (in mM): 205 sucrose, 5 KCl, 1.2 NaH_2PO_4, 26 $NaHCO_3$, 2.4 sodium/pyruvate, 1.3 L-ascorbic acid, 20 dextrose, 0.2 $CaCl_2$, and 1.3 $MgSO_4$ (290–300 mOsm, bubbled with 95% O_2 and 5% CO_2). Coronal brainstem slices (400–500 μM thick) at the level of the IC were sectioned using a Vibratome. The central nucleus of the IC was microdissected (Faye-Lund and Osen, 1985) and placed in Leibovitz's L-15 medium (Life Technologies, Gaithersburg, MD) containing papain (20 U/ml; Worthington, Lakewood, NJ) and bubbled with 100% oxygen for 45–60 min at 30–32 °C. The enzyme was washed with Leibovitz's L-15 medium containing ovomucoid inhibitor-albumin (1 mg/ml; Worthington, Lakewood, NJ). Neurons were then dissociated by gentle trituration with a fire-polished Pasteur pipette in Neurobasal-A (Life Technologies, Gaithersburg, MD) medium supplemented with 2% B27 (Life Technologies, Gaithersburg, MD), and penicillin (100 U/ml)-streptomycin (0.1 mg/ml). The dissociated IC neurons were then plated onto concanavalin A (100 mg/ml) or poly-D-lysine (50 μg/ml) coated glass coverslips for at least two hours prior to the start of patch-clamp experiments. Acutely dissociated IC neurons had round soma (15–25 μm in diameter) without processes.

2.3. Electrophysiology

The currents through Ca^{2+} channels were recorded at room temperature using the whole cell configuration of the patch-clamp techniques (Hamill et al., 1981). The patch electrodes were made from borosilicate glass capillaries and had resistances which ranged from 3 to 4 Ω M when filled with a solution containing (in mM): 90 cesium methanesulfonate, 10 EGTA, 30 phosphocreatine disodium, 10 HEPES, 10 glucose, 4 Na_2-ATP, 5 $MgCl_2$ and 0.4 Na-GTP (pH 7.3 with CsOH). Whole cell configuration was established in tyrode solution containing (in mM): 145 NaCl, 5.4 KCl, 2 $CaCl_2$, 1 $MgCl_2$, 10 HEPES, 10 glucose (pH 7.4 with NaOH), and the extracellular recording solution for isolating barium (Ba^{2+}) currents contained (in mM): 5 $BaCl_2$, 130 TEACl, 10 HEPES, 1 $MgCl_2$, 20 $CsCl_2$, 10 glucose and 0.001 TTX (pH 7.4 with TEAOH). Although Ca^{2+} is the biological charge carrier through Ca^{2+} channels, Ba^{2+} was used as a more reliable method for characterization of Ca^{2+} channel currents because Ba^{2+} permeates as well as Ca^{2+}, but does not inactivate the channel as it permeates through and in addition suppresses the residual K^+ currents. Voltage clamp experiments were performed with a Dagan 8900 patch-clamp amplifier. A liquid junction potential between the intracellular and extracellular solutions of ~11 mV, measured under current clamp mode (Neher, 1992) and calculated with Clampex, was corrected off-line. Currents were filtered at 10 kHz and whole cell capacitance was compensated. A series resistance compensation of ~80% was applied and monitored throughout recordings. Leak and residual capacitance currents were subtracted on-line using a $-P/n$ protocol (PClamp V6.0, Molecular Devices, Inc, Union City). Data were collected using Clampex 6.0 (Molecular Devices, Inc, Union City, CA) and analyzed off-line using Clamp fit and OriginPro 8.0 (Origin Lab Corp, Northampton, MA) softwares. For pharmacological tests, rapid external solution exchanges were performed to deliver Ca^{2+} channel blockers (Cleemann and Morad, 1991). The recording chamber was continuously perfused with the external solution and Ca^{2+} channel blockers were delivered to the neuron by an electronically controlled multi-barreled puffing device, which enables a rapid localized application of test solutions and their washout. The speed of external solutions exchange was <50 ms. The effects of Ca^{2+} channel blockers were tested after obtaining 2–5 min of steady control recordings. The Ca^{2+} channel toxins ω-agatoxin TK, ω-conotoxin GIVA, and SNX 482 were purchased from Alomone labs (Jerusalem, Israel), while nifedipine and nimodipine were obtained from Calbiochem (San Diego, CA). The solutions of Ca^{2+} channel toxins were prepared as concentrated stock solutions in distilled water and stored in 1 ml aliquots at −20 °C, in the dark, for less than 4 weeks. Stock solutions were diluted >1:1000 with the extracellular recording solution before each experiment. Cytochrome *C* (0.01%) was added to the ω-agatoxin TK, ω-conotoxin GIVA and SNX 482 solutions to saturate any nonspecific binding sites located on the walls of the tubing and chamber, which when applied alone had no effect on Ba^{2+} currents (data not shown). Nifedipine and nimodipine were solubilized in 100% ethanol as concentrated stock solutions and protected from ambient light at all times and stored in 1 ml aliquots at −20 °C. When diluted into the recording solution at ~18 mM, ethanol was without effect on Ba^{2+} currents in IC neurons (data not shown). All experiments were performed at room temperature (22–25 °C).

2.3.1. Voltage protocols

IC neurons were held at −80 mV and HVA Ba^{2+} currents were activated by step depolarization to 0 mV, following a 0.5 s conditioning pulse to −60 mV to inactivate the low threshold voltage-activated (LVA) Ca^{2+} channels; this protocol was applied at 0.1 Hz (Fig. 1A). Peak Ba^{2+} currents were measured at 5 ms into the test pulse. To generate current–voltage (*I–V*) relations, currents were evoked by using depolarization pulses of 50 ms from a holding potential (HP) of −90 mV (depolarization range: −90 mV to +60 mV at 10 mV increments). Data corresponding to the growth of Ca^{2+} currents from −60 mV to voltage corresponding to the peak current were fit with a Boltzmann function $I(V) = I_{max}/1 + e^{|(V_{1/2}-V)/S|}$, where I_{max} is the maximum current, V is the voltage, $V_{1/2}$ the voltage at half-maximal activation and S the slope of the curve (Almanza et al., 2007). To generate steady-state activation curves, the conductance ($G = I/[V - V_{rev}]$) was determined at each potential (V) and the reversal potential (V_{rev}) of the current was measured from the *I–V* curves (see Fig. 2). Normalized conductance was then plotted as a function of the test pulse and data were fit with a Boltzmann equation, $G/G_{max} = 1/(1 + e^{[(V-V_{1/2})/k]})$, where G_{max} is maximum conductance, $V_{1/2}$ is the voltage eliciting half-maximal G and k is the slope factor of activation. The steady-state inactivation of HVA Ba^{2+} currents was measured using a double-pulse protocol. A 0.5 s conditioning pulse preceded each depolarization at potentials between −100 mV and +30 mV followed by a 50 ms test pulse to 0 mV. Test currents were normalized to their maxima and plotted as a function of conditioning voltage. The data were then fit with a Boltzmann equation, $I/I_{max} = 1/(1 + e^{[(V-V_{1/2})/k]})$, where I/I_{max} is the normalized current, V is voltage in mV, $V_{1/2}$ is the voltage giving half-maximal inactivation, and k is the slope factor of inactivation. The kinetics of Ba^{2+} current inactivation was measured by using the ratio between the current amplitude at the end of the 0.5 s prepulse and the peak current amplitude ($R_{e/p}$); this parameter represents an inverse index of the current decay. To measure the kinetics of current activation (rise-time), the data were fit with a single exponential function, $I = A[1 - \exp(-t/\tau) + C$, where I is the current, A is the percentage of activation with time constant τ, t is the time, and C is the steady-state pedestal.

2.3.2. Data analysis

Currents were normalized relative to the membrane capacitance as an estimate of current density. Data obtained in SN-GEPR-3s were compared to control SD rats to determine changes in HVA Ca^{2+} channel currents associated with seizure

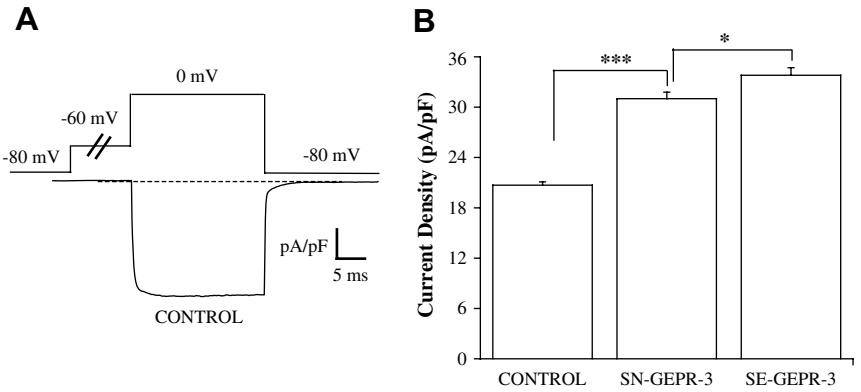

Fig. 1. Upregulation of Ca^{2+} channel currents in IC neurons of the GEPR-3s. A. Representative whole cell Ba^{2+} current trace in IC neuron of control SD rat. High threshold voltage-activated Ba^{2+} currents were activated by voltage steps to 0 mV, following a 0.5 s conditioning pulse to −60 mV to inactivate LVA channels, from the holding potential of –80 mV. B. The current density was significantly enhanced in IC neurons of SN-GEPR-3s ($n = 29$) compared to control SD rats ($n = 34$). Additional increases in current density were found in IC neurons of SE-GEPR-3s ($n = 19$) compared to SN-GEPR-3s ($n = 29$). $^{*}P < 0.05$, $^{***}P < 0.001$.

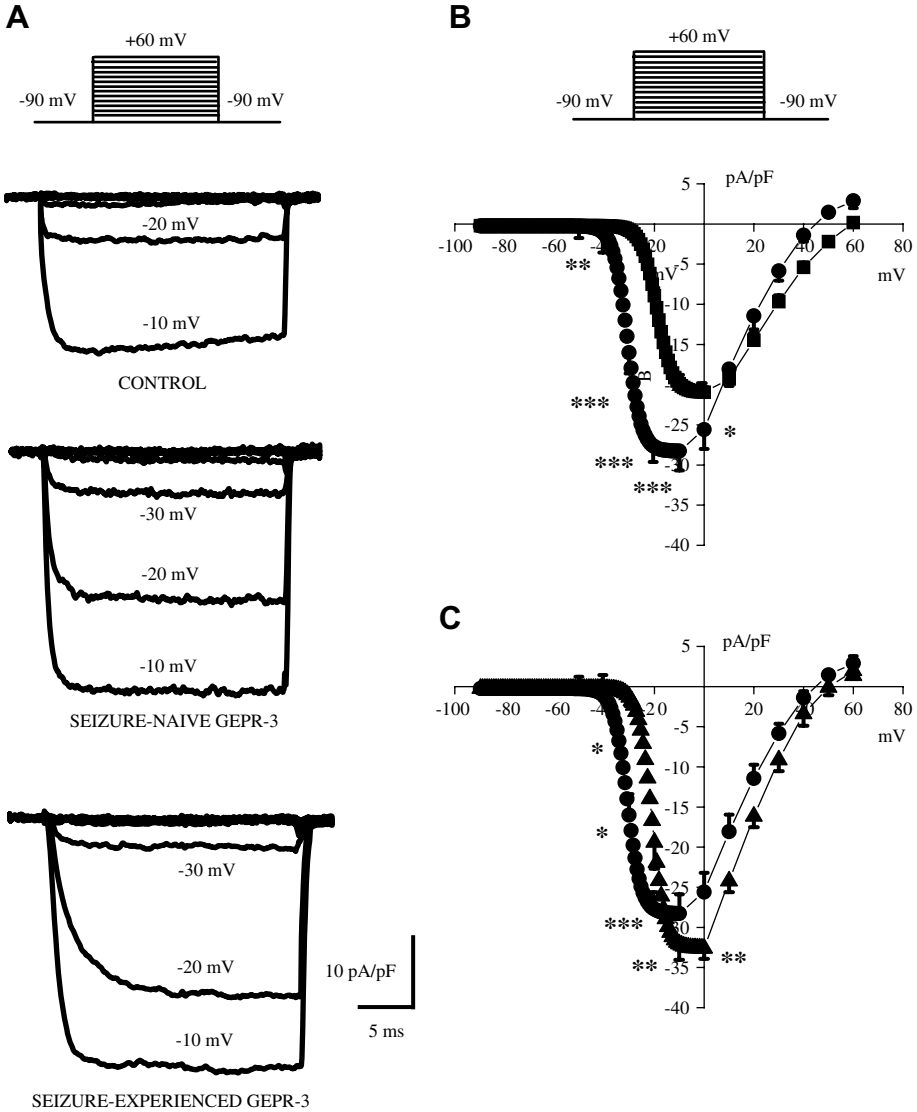

Fig. 2. Altered voltage-dependence of Ca^{2+} channel currents in IC neurons of the GEPR-3s. A. Representative Ba^{2+} current traces activated at different potentials in IC neurons from control SD rat (upper traces), SN-GEPR-3 (middle traces) and SE-GEPR-3 (lower traces). B. Voltage-dependence (*I–V*) of Ba^{2+} currents in IC neurons from control SD rats (filled squares, $n = 18$), SN-GEPR-3s (filled circles, $n = 15$) and SE-GEPR-3s (filled triangles, $n = 9$). Current density was fitted by a Boltzmann function. $^{*}P < 0.05$, $^{**}P < 0.01$, $^{***}P < 0.001$.

susceptibility whereas findings in SE-GEPR-3s were compared to SN-GEPR-3s to assess changes due to a single episode of reflex audiogenic seizure. Neurons exhibiting Ba^{2+} current "rundown" (>20% of the initial amplitude) within the first 5 min after membrane rupture and those with poor voltage control (i.e., slow tail currents) were excluded from the analysis. The inclusion of phosphocreatine in the patch pipettes effectively reduced the rundown of Ba^{2+} currents. The blocked (or sensitive) current was obtained by subtracting the current recorded under the Ca^{2+} channel blocker from that measured in control solutions immediately prior the blocker. Data were first subjected to normality test (Shapiro-Wilk) and test for homogeneity of variance (Levene's test and Brown–Forsythe's test) before the one-way analysis of variance (ANOVA). Differences between two groups with $P < 0.05$ were considered as statistically significant. The illustrated current traces represent the average of 3–5 consecutive traces and all data are presented as mean ± S.E.M.

3. Results

3.1. Enhanced Ca^{2+} channel currents in IC neurons of GEPR-3

Under control condition using Ba^{2+} extracellular solutions, depolarization steps to 0 mV from holding potential of −80 mV elicited an inward current (Fig. 1A). The current was identified as Ba^{2+} current entering IC neurons through voltage-dependent Ca^{2+} channels and will be referred to as Ca^{2+} channel current. Seizure-naive GEPR-3s used in this study as controls for SE-GEPR-3s displayed significant larger current density of HVA Ca^{2+} channels than control SD rats (control SD rats: -20.7 ± 0.4 pA/pF, $n = 34$; SN-GEPR-3s: -31.0 ± 0.8 pA/pF, $n = 29$; $F = 173.9$, $P < 0.001$; Fig. 1B). The current density also was significantly increased in SE-GEPR-3s compared to SN-GEPRs (SE-GEPR-3s: -33.8 ± 0.9 pA/pF, $n = 19$; SN-GEPR-3s: -31.0 ± 0.8 pA/pF, $n = 29$; $F = 6.27$, $P < 0.05$, Fig. 1B). The enhancement of HVA Ca^{2+} channel current density was not the result of increased cell capacitance (control SD rats: 84 ± 6 pF, $n = 34$; SN-GEPR-3s: 84 ± 5 pF, $n = 29$; SE-GEPR-3s: 85 ± 4 pF, $n = 19$). Fig. 2 quantifies the voltage-dependence of total Ca^{2+} channel current density in control SD rats ($n = 18$), SN-GEPR-3s ($n = 15$) and SE-GEPR-3s ($n = 9$). The original traces of Ca^{2+} channel currents from three representative neurons showed significant enhancement of the current density in SN-GEPR-3s compared to control SD rats (Fig. 2A). Quantification of current density at larger range of voltages (−90 mV to +60 mV) showed that Ca^{2+} channel currents appear to activate at −40 mV, −60 mV and −40 mV and peaked at 0 mV, −20 mV and −10 mV in control SD rats, SN-GEPR-3s and SE-GEPR-3s, respectively (Fig. 2B). The current density of Ca^{2+} channels was enhanced between −40 mV and −10 mV, as if there was a −20 mV shifts in *I–V* relations in SN-GEPR-3s, with little or no change in the current at positive voltages, as compared to control SD rats. Comparisons of *I–V* relations of total Ca^{2+} channel current density between SE-GEPR-3s and SN-GEPR-3s, showed significant enhancement of the current density in SE-GEPR-3s at −10 mV and 0 mV, but also significant decreases between −40 mV and −20 mV (Fig. 2C). Quantification also shows that half-maximal voltage was significantly enhanced in IC neurons of SN-GEPR-3s (-30.9 ± 2.3 mV and 3.3 ± 0.2 mV, $n = 15$, $F = 20.3$; $P < 0.001$; Fig. 2C) compared to control SD rats (-18.6 ± 1.1 mV and 2.8 ± 0.2 mV, $n = 20$). In SE-GEPR-3s, the half-maximal voltage was significant decreased (-21 ± 1 mV and 2.7 ± 0.3 mV, $n = 9$; $F = 6.8$; $P < 0.01$; Fig. 2C) compared to SN-GEPR-3s (-30.9 ± 2.3 mV and 3.3 ± 0.2 mV, $n = 15$). Thus, there appears to be both enhancement

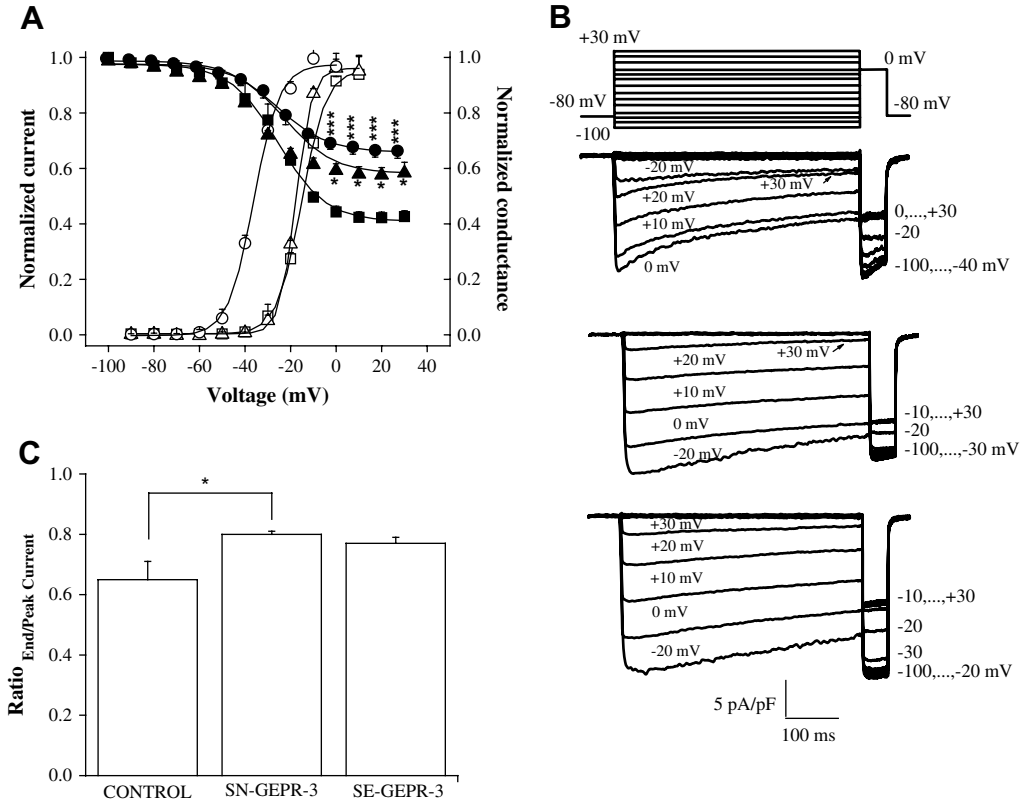

Fig. 3. Altered gating parameters of Ca^{2+} channels in IC neurons of the GEPR-3s. A. Voltage-dependent activation and steady-state inactivation of Ba^{2+} currents in control SD rats, SN-GEPR-3s, and SE-GEPR-3s. Steady-state inactivation was measured using a 0.5 s prepulse, as illustrated in panel B. Data from each cell were fitted with a Boltzmann equation. Ba^{2+} currents did not completely inactivate in IC neurons obtained from control SD rats ($n = 9$, filled squares), SN-GEPR-3s ($n = 8$, filled circles) and SE-GEPR-3s ($n = 9$, filled triangles). The steady-state conductance (G) was transformed from *I–V* data shown in Fig. 2B. The curves are fits of the data to a Boltzmann equation. The activation curve was significantly shifted towards negative voltages in SN-GEPR-3s ($n = 15$, open circles), as compared to control SD rats ($n = 21$, open squares) and SE-GEPR-3s ($n = 9$, open triangles). B. Representative traces of Ba^{2+} currents to construct the steady-state inactivation curves in IC neuron from control SD rat (upper panel), SN-GEPR-3 (middle panel) and SE-GEPR-3 (lower panel). C. The ratio between the current amplitude at the end of the 0.5 s pulse and the peak current amplitude ($R_{e/p}$) was significantly higher in IC neurons obtained from SN-GEPR-3s ($n = 8$) compared to control SD rats ($n = 9$). *$P < 0.05$.

of the Ca^{2+} channel current density and altered channel gating parameters in SN-GEPR-3s compared to control SD rats, as well as in SE-GEPR-3s compared to SN-GEPR-3s. It should be pointed out that the magnitude of the current activated at voltages between −90 mV and −50 mV in all three groups was significantly smaller, as compared to the current at voltages >−50 mV, indicative of smaller expression of LVA Ca^{2+} channels in IC neurons.

3.2. Gating parameters of Ca^{2+} channels are altered in IC neurons of the GEPR-3

Fig. 3 (panel A) shows activation and steady-state inactivation curves for Ca^{2+} channel currents measured in IC neurons obtained from control SD rats, SN-GEPR-3s, and SE-GEPR-3s. SN-GEPR-3s exhibited a significant −20 mV shifts in the half-maximal activation voltage relative to the control group (SN-GEPR-3s: -37 ± 2 mV and 2.9 ± 0.2 mV, $n = 15$; control SD rats: -15 ± 1 mV and 3.8 ± 0.2 mV, $n = 21$, $P < 0.05$). Interestingly, the negative shift in current activation observed in SN-GEPR-3s (-37 ± 2 mV and 2.9 ± 0.2 mV, $n = 15$) was fully reversed by seizure episodes in SE-GEPR-3s (-19 ± 1 mV and 3.5 ± 0.3 mV, $n = 9$ compared to control SD rats: -15 ± 1 mV and 3.8 ± 0.2 mV, $n = 21$). Fig. 3 (panel B) also shows that conditioning depolarizing pulses in the range of −100 mV to +30 mV applied in 10 mV steps failed to inactivate the current evoked at 0 mV in IC neurons. Conditioning pulses as long as 5 s failed to cause additional inactivation of the current (data not shown), indicating that the conditioning pulse used here is of sufficient duration. SN-GEPR-3s and control SD rats showed no difference in either the half-maximal voltage or the slope factor of steady-state inactivation (control SD rats: -25 ± 1 mV and 9 ± 1 mV, $n = 9$; SN-GEPR-3s: -23 ± 2 mV and 8 ± 1 mV, $n = 8$; $P < 0.2$). The half-maximal voltage also was not significant altered in SE-GEPR-3s (-25 ± 1 mV and 11 ± 1 mV, $n = 9$; $P < 0.3$) compared to SN-GEPR-3s (-23 ± 2 mV and 8 ± 1 mV, $n = 8$; Fig. 3). However, we observed significant differences in the fraction of non-inactivating current (Fig. 3B). The non-inactivating current was significantly increased from $45 \pm 5\%$ ($n = 9$) in control SD rats to $72 \pm 2\%$ in SN-GEPR-3s ($n = 8$; Fig. 3A; $F = 19.5$, $P < 0.001$). In

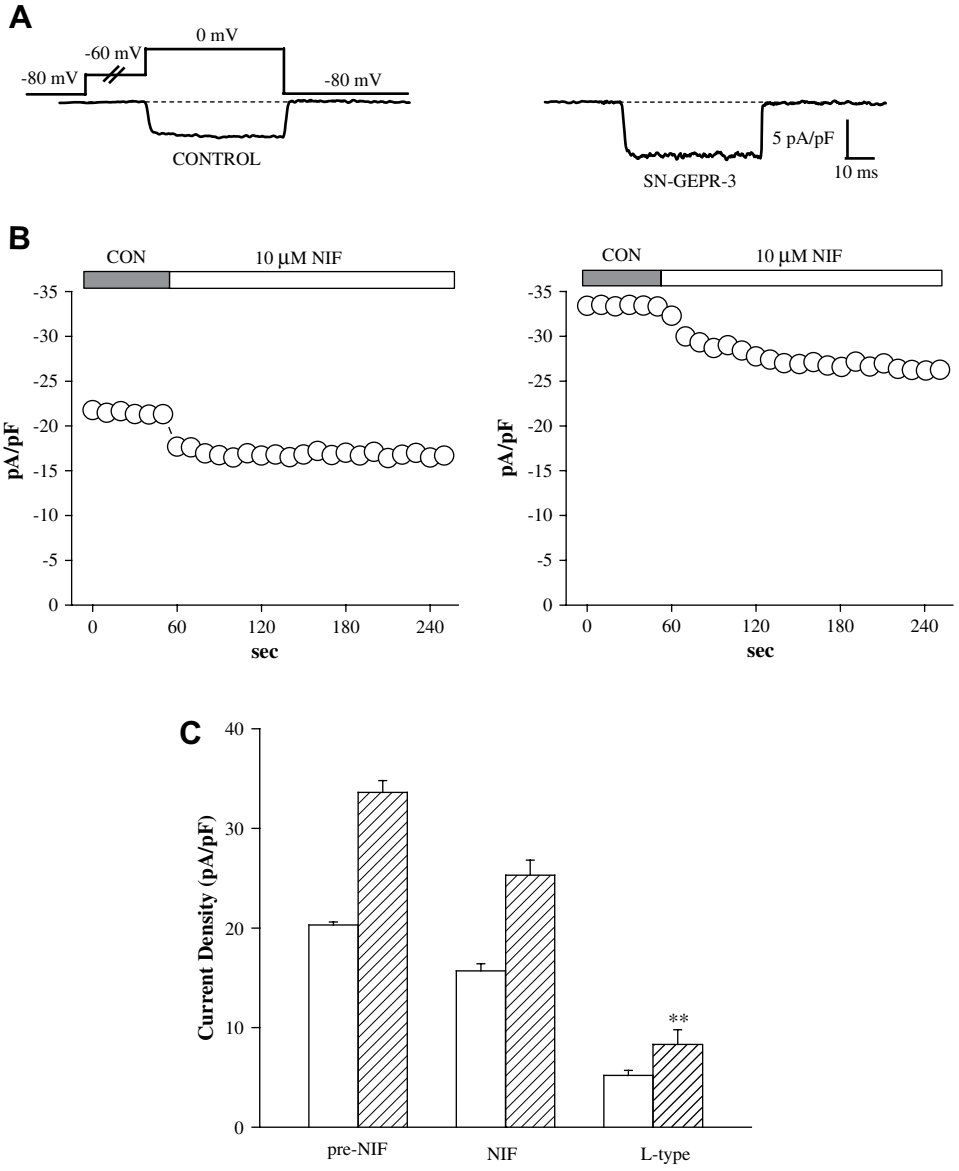

Fig. 4. Enhancement of L-type current density in IC neurons of SN-GEPR-3s. Ba^{2+} currents were activated at 0 mV in absence and presence of 10 μM nifedipine in IC neurons obtained from control SD rats and SN-GEPR-3s. A. Representative nifedipine-sensitive current trace (difference current in the presence and absence of nifedipine) in control SD rat (left trace) and SN-GEPR-3 (right trace). B. Time course of the suppressive effect of nifedipine on HVA Ca^{2+} channel currents in control SD rat (left panel) and SN-GEPR-3 (right panel). C. Nifedipine-sensitive current (10 μM, L-type) was larger in SN-GEPR-3s ($n = 8$) compared to control SD rats ($n = 10$). $^{**}P < 0.01$.

SE-GEPR-3s, the non-inactivating fraction of the current was significantly decreased (58 ± 3%, $n = 9$; Fig. 3A; $F = 15.7$, $P < 0.001$) compared to SN-GEPR-3s (72 ± 2%, $n = 8$). We also examined the kinetics of inactivation by measuring the ratio $R_{e/p}$ of the conditioning pulse at 0 mV (Fig. 3C). Quantification shows that SN-GEPR-3s had significantly higher $R_{e/p}$ values (slow current decay) compared to controls SD rats (SN-GEPR-3s: 0.8 ± 0.01, $n = 8$; SD rats: 0.65 ± 0.06; $n = 9$; $F = 5.65$, $P < 0.05$). No significant change in $R_{e/p}$ values was found between SN-GEPR-3s (0.8 ± 0.01, $n = 8$) and SE-GEPR-3s (0.77 ± 0.02, $n = 9$; $P < 0.3$). The time constant (τ) of activation (rise-time) measured at 0 mV did significantly not differ between SN-GEPR-3s (0.6 ± 0.1 ms, $n = 15$) and control SD rats (0.8 ± 0.1 ms, $n = 21$; $P < 0.2$) as well as between SE-GEPR-3s (0.6 ± 0.1 ms, $n = 9$) and SN-GEPR-3s (0.6 ± 0.1 ms, $n = 15$; $P < 0.5$).

3.3. Which HVA Ca^{2+} channel types contribute to the increased current in IC neurons of GEPR-3?

The contribution of different types of HVA Ca^{2+} channels to enhancement of total Ba^{2+} current density in IC neurons of SN-GEPR-3s was quantified using selective pharmacological blockers of L-, N-, P/Q-, and R-type Ca^{2+} channels (Figs. 4–8). Because the current density was increased only by ~10% in SE-GEPR-3s compared to SN-GEPR-3s, the pharmacological studies were only performed using SN-GEPR-3s. Quantification of the current sensitive to nifedipine (10 μM) indicated that L-type current density was significantly increased in IC neurons of SN-GEPR-3s (8.3 ± 1.5 pA/pF, $n = 8$, compared to the control SD rats: 4.9 ± 0.5 pA/pF, $n = 10$; $F = 5.9$, $P < 0.05$, Fig. 4). Similarly, the nimodipine-sensitive current (1 μM, L-type) also was enhanced significantly in IC neurons of SN-GEPR-3s (7.4 ± 0.4 pA/pF, $n = 6$, compared to the control SD rats: 4.7 ± 0.4 pA/pF, $n = 6$; $F = 21.1$, $P < 0.01$, Fig. 5). Significant increases in the ω-conotoxin-sensitive current density (1 μM, N-type) also were found in IC neurons of SN-GEPR-3s (9.6 ± 1.3 pA/pF, $n = 8$, compared to the control SD rats: 5.5 ± 0.9 pA/pF, $n = 9$, $F = 7.4$, $P < 0.01$; Fig. 6). The SNX 482-sensitive current (100 nM, R-type) also was significantly increased in IC neurons of SN-GEPR-3s (10.3 ± 1.4 pA/pF, $n = 8$, compared to the control SD rats: 4.9 ± 0.9 pA/pF, $n = 8$; $F = 20.3$, $P < 0.01$; Fig. 7). In contrast, no significant change in the 30 nM ω-agatoxin TK-sensitive current

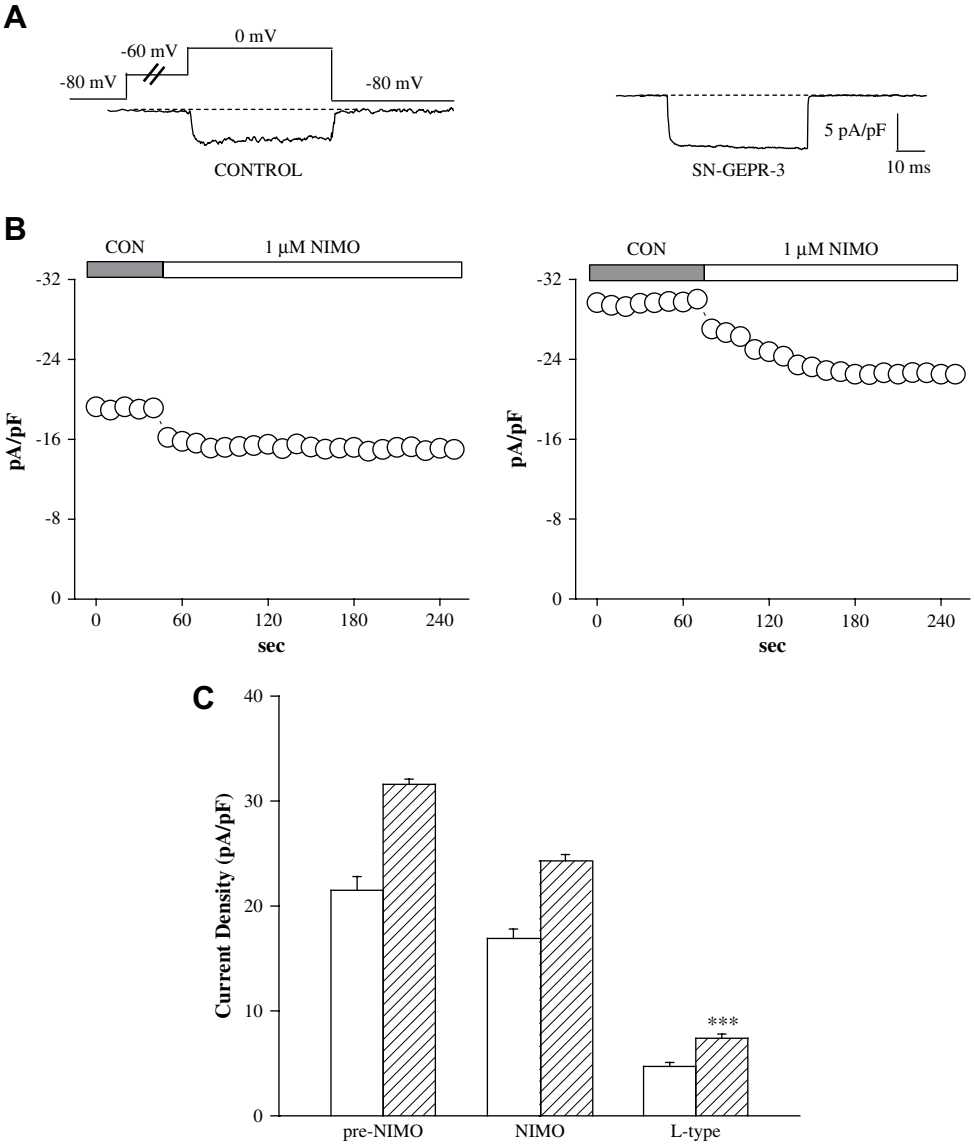

Fig. 5. Enhancement of L-type current density in IC neurons of SN-GEPR-3s. Ba^{2+} currents were activated at 0 mV in absence and presence of 1 μM nimodipine in IC neurons obtained from control SD rats and SN-GEPR-3s. A. Representative nimodipine-sensitive current trace (obtained as described in Fig. 4A) in control SD rat (left trace) and SN-GEPR-3 (right trace). B. Time course of the suppressive effect of nimodipine on HVA Ca^{2+} channel currents in control SD rat (left panel) and GEPR-3 (right panel). C. Nimodipine-sensitive current (10 μM, L-type) was larger in SN-GEPR-3s ($n = 6$) compared to control SD rats ($n = 6$). ***$P < 0.001$.

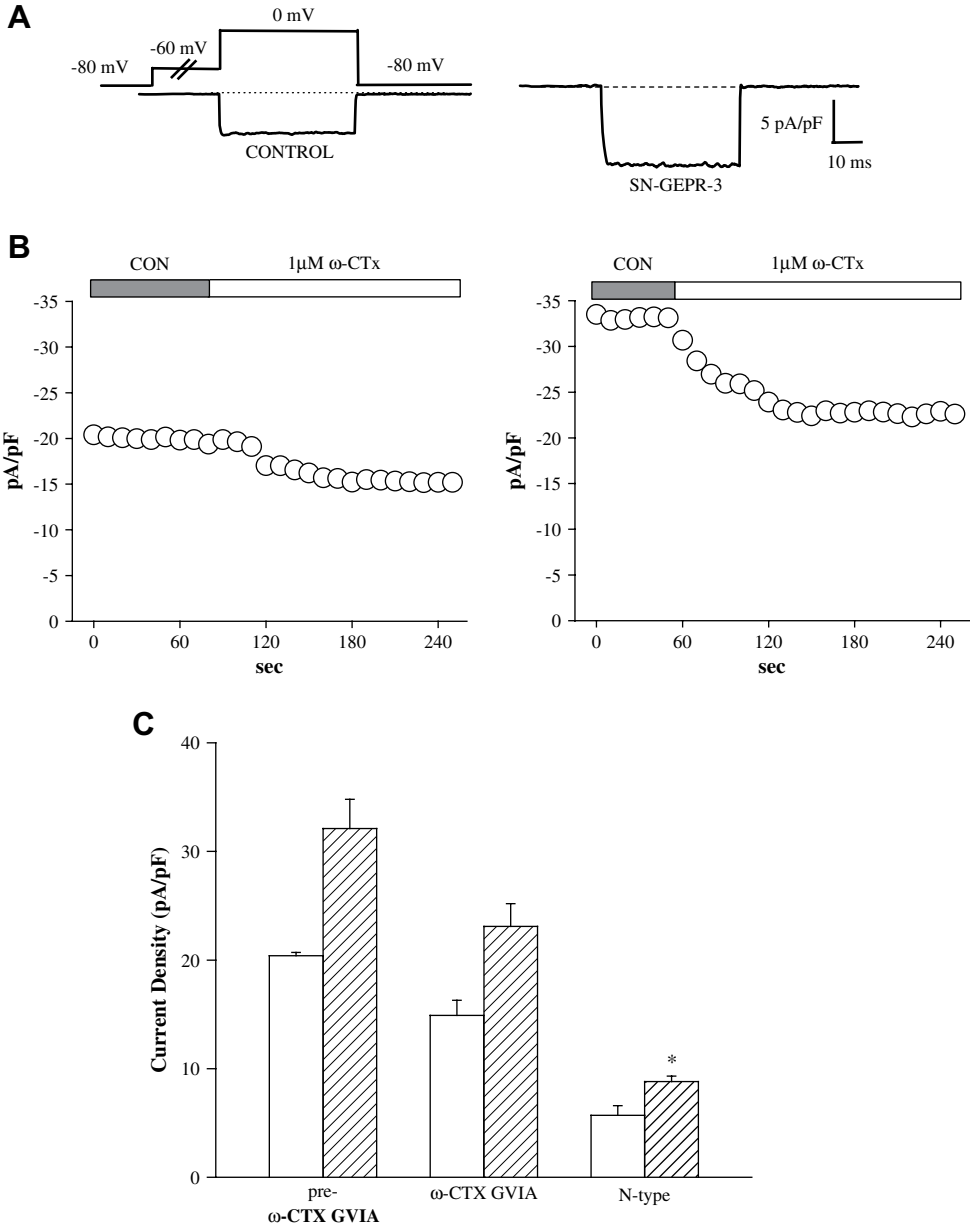

Fig. 6. Enhancement of N-type current density in IC neurons of SN-GEPR-3s. Ba^{2+} currents were activated at 0 mV in absence and presence of 1 μM ω-conotoxin GVIA in IC neurons obtained from control SD rats and SN-GEPR-3s. A. Representative ω-conotoxin GVIA-sensitive current trace (obtained as described in Fig. 4A) in control SD rat (left trace) and SN-GEPR-3 (right trace). B. Time course of the suppressive effect of ω-conotoxin GVIA on HVA Ca^{2+} channel currents in control SD rat (left panel) and SN-GEPR-3 (right panel). C. The ω-conotoxin GVIA-sensitive current was larger in SN-GEPR-3s ($n = 8$) compared to control SD rats ($n = 9$). $^*P < 0.05$.

(P-type) was found in IC neurons of SN-GEPR-3s (4.5 ± 0.4 pA/pF, $n = 8$, compared to control SD rats: 4.6 ± 0.3 pA/pF, $n = 7$; Fig. 8). Q-type current was quantified by incubating the IC neurons first in 30 nM ω-agatoxin TK that blocks P-type channels and then exposing the cells to 200 nM of the same toxin. This approach suggests no significant change in Q-type current density in IC neurons of SN-GEPR-3s (7.2 ± 1.1 pA/pF, $n = 8$, compared to control SD rats: 6.1 ± 0.7 pA/pF, $n = 7$; Fig. 5B). It should be noted that the sum of current inhibited by the above Ca^{2+} channel blockers exceeds the total current by ~25% suggesting possible redundancy of blocker specificity as previously reported (McDonough et al., 2002).

4. Discussion

The major finding of this report is that HVA Ca^{2+} channel current density is enhanced in IC neurons of seizure-naive GEPR-3s compared to control animals. This increase was accompanied with change in the voltage-dependence of Ca^{2+} channel activation curves as well as lower current decay and significant increases in the non-inactivating fraction of channels. Pharmacological analyses revealed that increased contribution of L-, N- and R-type Ca^{2+} channels accounts for enhancement of the current density in SN-GEPR-3s. Seizure episodes in the GEPR-3s further enhanced the current density but appear to normalize the gating properties of Ca^{2+} channels. Since IC neurons are thought to be critical in the initiation of reflex audiogenic seizures in the GEPRs, the chronic upregulation of HVA current density and large shifts in the activation voltage of Ca^{2+} channel may underlie their proclivity to seizures.

4.1. Seizure susceptibility and enhancement of Ca^{2+} channel current density in IC neurons

Ca^{2+}-dependent mechanisms are thought to play an important role in seizure generation (Sanabria et al., 2001). Consistent with

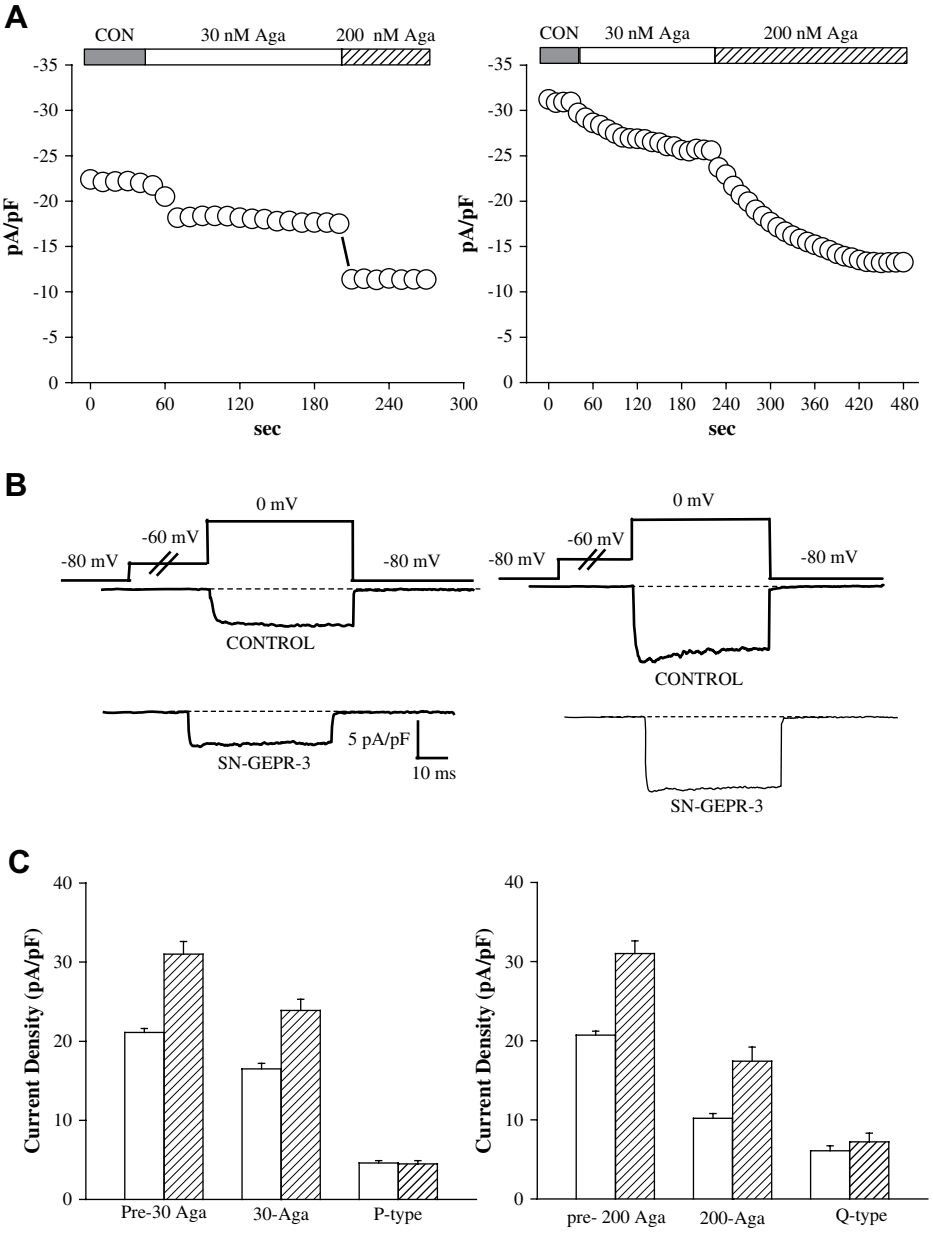

Fig. 7. P- and Q-type current densities are not enhanced in IC neurons of SN-GEPR-3s. Ba^{2+} currents were activated at 0 mV in absence and presence of ω-agatoxin TK in IC neurons obtained from control SD rats and SN-GEPR-3s. A. Time course of the suppressive effect of 30 nM (P-type) and 200 nM (Q-type) ω-agatoxin TK currents in control SD rat (left panel) and SN-GEPR-3 (right panel). B. The representative 30 nM ω-agatoxin TK-sensitive current traces (P-type, left panel; control SD rat: upper trace; SN-GEPR-3: lower trace) and 200 nM ω-agatoxin TK-sensitive current traces (Q-type, right panel; control SD rat: upper trace; SN-GEPR-3: lower trace) were obtained as described in Fig. 4A. C. The 30 nM ω-agatoxin TK-sensitive current (P-type, left panel) was not altered in IC neurons of SN-GEPR-3s ($n = 8$) compared to control SD rats ($n = 7$). The 200 nM ω-agatoxin TK-sensitive current (Q-type, right panel) also was not significantly altered in IC neurons of SN-GEPR-3s ($n = 8$) compared to control SD rats ($n = 7$).

this idea, HVA Ca^{2+} current density was larger in IC neurons of the GEPR-3s. The increase in HVA Ca^{2+} channel currents also has been reported in various acquired models of generalized seizures and epilepsy including kindling epileptogenesis and kainate post-status epilepticus model of limbic epilepsy (Vreugdenhil and Wadman, 1992; Beck et al., 1998). The specific role of each subtype of HVA Ca^{2+} channel currents has not been quantified in these models of temporal lobe epilepsy, although enhancement of N- and L-type current has been suggested in kindling (Vreugdenhil and Wadman, 1992; Wang et al., 2007). In the pilocarpine model of post-status epilepticus N-type current was decreased in hippocampus CA1 neurons even though LVA currents were upregulated (Su et al., 2002). N-type current may also be altered in IC neurons of the GEPR-9s, which exhibits the most severe form of reflex audiogenic seizures (Li et al., 1994). In rats with genetically determined absence-like seizures, LVA but not HVA currents were upregulated in reticular thalamic neurons (Tsakiridou et al., 1995). Unlike this model of generalized non-convulsive epilepsy, alcohol withdrawal seizures were accompanied by upregulation of L- and P-type but not of LVA currents in IC neurons (N'Gouemo and Morad, 2003a). Since the enhanced HVA Ca^{2+} channel currents in SN-GEPR-3s also included the L-type current, it appears that upregulation of this current type may be a common mechanism underlying neuronal hyperexcitability in models of reflex generalized clonic seizures. Evidence suggests that R-type channel plays an important role in the generation of seizures as ablating gene encoding for R-type channel reduced the incidence of generalized seizures and prevented seizure generalization (Suzuki et al., 2004; Weiergraber et al., 2006, 2007). Interestingly, we found that R-type current density was the most elevated HVA Ca^{2+} channel currents in IC

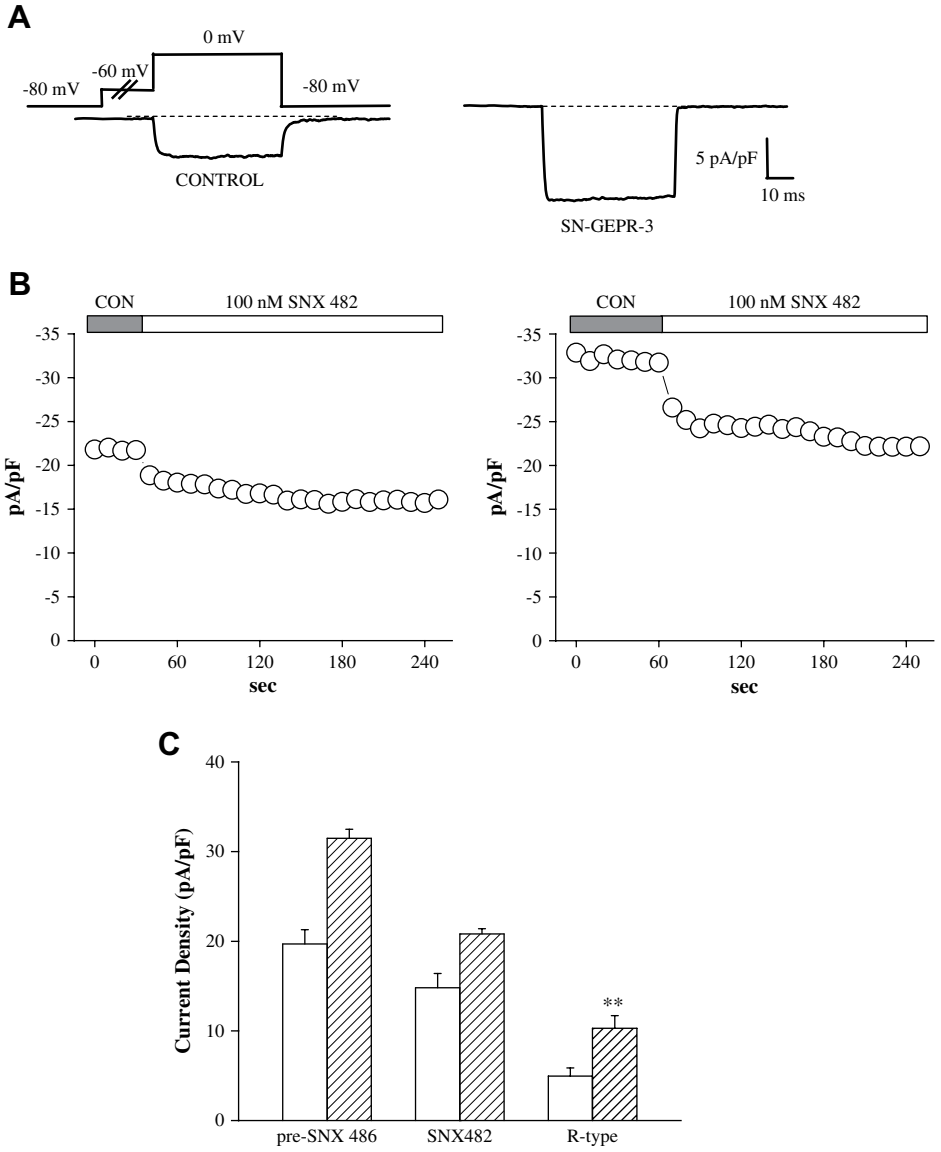

Fig. 8. Enhancement of R-type current density in IC neurons of SN-GEPR-3. Ba^{2+} currents were activated at 0 mV in absence and presence of 100 nM SNX 482 in IC neurons obtained from control SD rats and SN-GEPR-3s. A. Representative SNX 482-sensitive current traces (obtained as described in Fig. 4A) in control SD rat (left trace) and SN-GEPR-3 (right trace). B. Time course of the suppressive effect of SNX 482 on HVA Ca^{2+} channel currents in control SD rat (left panel) and SN-GEPR-3 (right panel). C. SNX 482-sensitive current (R-type) was larger in SN-GEPR-3s ($n = 8$) compared to control SD rats ($n = 8$). $^{**}P < 0.01$.

neurons of SN-GEPR-3s. Because R-type current appears to activate around −50 mV in IC neurons (N'Gouemo and Morad, 2003b), it is likely that this current may contribute to the observed leftward shift in current activation curve.

4.2. Mechanisms underlying increased Ca^{2+} channel current density in IC neurons of GEPR-3

The increase in HVA Ca^{2+} channel current density was not associated with significant changes in the levels of protein expression of the pore-forming α1 subunit of some types of HVA Ca^{2+} channels in SN-GEPR-3s and SE-GEPR-3s (N'Gouemo et al., 2003). This finding suggests that increases in N-, L- and R-type current density may be mediated by mechanisms that affect the gating of the channel such as negative shifts in activation voltages, slower current decay, and/or increases in the fraction of non-inactivating current. In the present study the absence of alteration in steady-state inactivation parameters of HVA Ca^{2+} channel currents in IC neurons of the GEPR-3s may be in part due to the use of Ba^{2+} as a charge carrier. Nevertheless, a slower current decay was found in IC neurons of the GEPR-3s, which may result in large availability of HVA Ca^{2+} channels and/or prolongation of mean channel open time. The mechanisms responsible for changes in inactivation kinetics of Ca^{2+} current remain unknown. The enhancement of HVA Ca^{2+} channel current density could also reflect a change in metabolic processes such as phosphorylation as is suggested indirectly from the significant shift in the peak of *I–V* relations in SN-GEPR-3s (Fig. 2B). In line with this hypothesis, focal microinjection of cyclic AMP derivatives within the IC has been reported to trigger audiogenic seizure susceptibility in normal rats and status epilepticus in the GEPR-9s (Ludvig and Moshé, 1989).

4.3. Increased current density of HVA Ca^{2+} related to neuronal hyperexcitability in GEPR-3s

Ca^{2+} channel antagonists are known to suppress reflex audiogenic seizures in the GEPR-3s (De Sarro et al., 1990) suggesting that Ca^{2+} channel expression and/or function may be altered at least in IC neurons of these animals. Consistent with this idea, our data showed increased HVA Ca^{2+} channel current density in IC neurons

of the GEPR-3s. The precise mechanisms of how enhancement of HVA Ca^{2+} channel current contributes to neuronal hyperexcitability and subsequent seizures are not well understood. Some types of Ca^{2+} channels are known to contribute to the activation of Ca^{2+}-activated potassium (K_{Ca}) channels, which initiate repolarization and afterhyperpolarization representing an intrinsic inhibitory mechanism (Alger and Nicoll, 1980; Jin et al., 2000; Brenner et al., 2005; Lappin et al., 2005). Hence, enhanced Ca^{2+} channel currents could therefore provide sufficient Ca^{2+} to trigger both Ca^{2+}-dependent inactivation of the channels and activation of K_{Ca} channels, thereby contributing to terminate the bursting activity that accompanies seizures. These mechanisms, however, also appear to be altered as K_{Ca} current density is reduced in IC neurons of SN-GEPR-3s, consistent with a marked reduction in spike frequency and magnitude of afterhyperpolarization reported in hippocampus CA3 neurons of the GEPR-9s (Verma-Ahuja et al., 1995; N'Gouemo et al., 2006a). In this respect, we have already reported a downregulation of N-type Ca^{2+} channel protein that is thought to be limited to activation of K_{Ca} currents in alcohol withdrawal seizures (N'Gouemo et al., 2006b). In seizure-experienced GEPR-3s, shifts in the voltage-dependence of HVA Ca^{2+} channel currents were accompanied by a reduction of the current density at negative voltages compared to SN-GEPR-3s. Thus, it is likely that seizures may have reduced the expression of some types of HVA Ca^{2+} channels that would have been activated at voltages negative to or around −40 mV (i.e., L- and R-type). This reduction of HVA Ca^{2+} channel currents also could contribute to decrease K_{Ca} currents. Thus, chronic upregulation of HVA Ca^{2+} channel current density and downregulation of K_{Ca} current density may represent a cohesive mechanism that contributes to chronic IC neuronal hyperexcitability leading to enhanced seizure susceptibility in the GEPR-3s.

We conclude that the increased HVA Ca^{2+} channel current density due to large negative shifts in channel activation and slower rates of channel inactivation may contribute to chronic synaptic excitation, thus increasing neuronal excitability and the release of excitatory neurotransmitter, which in turn would promote a greater incidence of bursting activity in IC neurons of the GEPR-3s.

Acknowledgments

This study was supported by the National Institutes of Health Public Grants (NS047193 to P.N., AA11628 to C.L.F., and HL16152 to M.M.). The contents of this publication are the responsibility of the authors and do not necessarily represent the official views of the NIH. The authors are grateful to Drs. Einsley M. Janowski, Curtis F. Barrett and Ansalan Stewart for editorial help and valuable comments.

References

Alger, B.E., Nicoll, R.A., 1980. Epileptiform burst afterhyperpolarization: calcium-dependent potassium potential in hippocampal CA1 pyramidal cells. Science 210, 1122–1124.

Almanza, A., Navarrete, F., Vega, R., Soto, E., 2007. Modulation of voltage-gated Ca^{2+} current in vestibular hair cells by nitric oxide. Journal of Neurophysiology 97, 1188–1195.

Beck, H., Steffens, R., Elger, C.E., Heinemann, U., 1998. Voltage-dependent Ca^{2+}-current in epilepsy. Epilepsy Research 32, 321–332.

Brenner, R., Chen, Q.H., Vilaythong, A., Toney, G.M., Noebels, J.L., Aldrich, R.W., 2005. BK channel beta 4 subunit reduces dentate gyrus excitability and protects against temporal lobe seizures. Nature Neuroscience 18, 1752–1759.

Browning, R.A., 1986. Neuroanatomical localization of structures responsible for seizures in the GEPR: lesion studies. Life Science 39, 857–867.

Burgess, D.L., Jones, J.M., Meisler, M.H., Noebels, J.L., 1997. Mutation of the Ca^{2+} channel beta subunit gene Cchb4 is associated with ataxia and seizures in the lethargic (*lh*) mouse. Cell 88, 385–392.

Chakravarty, D.N., Faingold, C.L., 1998. Comparison of neuronal response patterns in the external and central nuclei of inferior colliculus during ethanol administration and ethanol withdrawal. Brain Research 783, 102–108.

Chioza, B., Wilkie, H., Nashef, L., Blower, J., McCormick, D., Sham, P., Asherson, P., Makoff, A.J., 2001. Association between the α_{1a} calcium channel gene CACNA1A and idiopathic generalized epilepsy. Neurology 56, 1245–1246.

Cleemann, L., Morad, M., 1991. Role of Ca^{2+} channel in cardiac excitation–contraction coupling in the rat: evidence from Ca^{2+} transients and contraction. Journal of Physiology 432, 283–312.

Dailey, J.W., Mishra, P., Ko, K.H., Penny, J.E., Jobe, P.C., 2001. Noradrenergic abnormalities in the central nervous system of seizure-naive genetically epilepsy-prone rat. Epilepsia 32, 168–173.

De Sarro, G., De Sarro, A., Federico, F., Meldrum, B.S., 1990. Anticonvulsant properties of some calcium antagonists on sound-induced seizures in genetically epilepsy-prone rats. General Pharmacology 21, 769–778.

Escayg, A., De Waard, M., Lee, D.D., Bichet, D., Wolf, P., Mayer, T., Johnston, J., Baloh, R., Sander, T., Meisler, M.H., 2000. Coding and noncoding variation of the human calcium channel β4-subunit gene CACNB4 in patients with idiopathic generalized epilepsy and episodic ataxia. American Journal of Human Genetics 66, 1531–1539.

Evans, M.S., Viola-McCabe, K.E., Caspary, D.M., Faingold, C.L., 1994. Loss of synaptic inhibition during repetitive stimulation in genetically epilepsy-prone rats (GEPR). Epilepsy Research 18, 97–105.

Faingold, C.L., 1999. Neuronal networks in the genetically epilepsy-prone rat. Advances in Neurology 79, 311–321.

Faingold, C.L., Gehlbach, G., Caspary, D.M., 1986. Decreased effectiveness of GABA-mediated inhibition in the inferior colliculus of the genetically epilepsy-prone rat. Experimental Neurology 93, 145–159.

Faingold, C.L., N'Gouemo, P., Riaz, A., 1998. Ethanol and neurotransmitter interactions – from molecular to integrative effects. Progress in Neurobiology 55, 509–535.

Faingold, C.L., Knapp, D.J., Chester, J.A., Gonzalez, L.P., 2004. Integrative neurobiology of the alcohol withdrawal syndrome – from anxiety to seizures. Alcoholism: Clinical and Experimental Research 28, 268–278.

Faye-Lund, H., Osen, K.K., 1985. Anatomy of the inferior colliculus in rat. Anatomy and Embryology 171, 1–20.

Fen, H.-J., Faingold, C.L., 2002. Repeated generalized audiogenic seizures induce plastic changes on acoustically evoked neuronal firing in the amygdala. Brain Research 932, 61–69.

Fletcher, C.F., Lutz, C.M., O'Sullivan, T.N., 1996. Absence epilepsy in tottering mutant mice is associated with calcium defects. Cell 87, 607–617.

Frye, G.D., McCown, T.J., Breese, G.R., 1983. Characterization of susceptibility to audiogenic seizures in ethanol-dependent rats after microinjection of gamma-aminobutyric acid (GABA) agonists into the inferior colliculus, substantia nigra or medial septum. Journal of Pharmacology and Experimental Therapeutics 227, 663–670.

Hamill, O.P., Marty, A., Neher, E., Sakmann, B., Sigworth, F.J., 1981. Improved patch-clamp techniques for high-resolution current recording from cells and cell-free membrane patches. Pflügers Archives-European Journal of Physiology 391, 85–100.

Jin, W., Sugaya, A., Tsuda, T., Oliguchi, H., Sugaya, E., 2000. Relationship between large conductance calcium-activated potassium channel and busting activity. Brain Research 860, 21–28.

Jobe, P.C., Browning, R.A., 2006. Mammalian models of genetic epilepsy characterized by sensory-evoked seizures and generalized seizure susceptibility. In: Pitkänen, A., Schwartzkroin, P.A., Moshé, S.L. (Eds.), Models of Seizures and Epilepsy. Elsevier, Amsterdam, pp. 261–271.

Jobe, P.C., Laird, H.E., 1981. Neurotransmitter abnormalities as determinants of seizure susceptibility and intensity in the genetic models of epilepsy. Biochemical Pharmacology 30, 3137–3144.

Jobe, P.C., Picchioni, A.L., Chin, L., 1973. Role of norepinephrine in audiogenic seizures in the rat. Journal of Pharmacology and Experimental Therapeutics 184, 1–10.

Jouvenceau, A., Eunson, L.H., Ramesh, V., Zuberi, S.M., Kullmann, D.M., Hanna, M.G., 2001. Human epilepsy associated with dysfunction of the brain P/Q-type calcium channel. Lancet 358, 801–807.

Lappin, S.C., Dale, T.J., Brown, J.T., Davies, G.H., 2005. Activation of SK channel inhibits epileptiform bursting in hippocampal CA3 neurons. Brain Research 1065, 37–46.

Li, Y., Evans, M.S., Faingold, C.L., 1994. Inferior colliculus neuronal membrane and synaptic properties in genetically epilepsy-prone rats. Brain Research 660, 232–240.

Little, H.J., Dolin, S.J., Hasley, M.J., 1986. Calcium channel antagonists decrease the ethanol the ethanol withdrawal syndrome. Life Science 39, 2059–2065.

Ludvig, N., Moshé, S.L., 1989. Different behavioral and electrographic effects of acoustic stimulation and dibutyryl cyclic AMP injection into the inferior colliculus in normal and in genetically epilepsy-prone rats. Epilepsy Research 3, 185–190.

McDonough, S.I., Boland, L.M., Mintz, I.M., Bean, B.P., 2002. Interactions among toxins that inhibits N-type and P-type calcium channels. Journal of General Physiology 119, 313–328.

N'Gouemo, P., Faingold, C.L., 1996. Repetitive audiogenic seizures caused an increased acoustic response in inferior colliculus neurons and additional convulsive behaviors in the genetically epilepsy-prone rats. Brain Research 710, 92–96.

N'Gouemo, P., Faingold, C.L., 1998. The periacqueductal gray neurons exhibit increased neuronal responsiveness associated with audiogenic seizures in the genetically epilepsy-prone rat. Neuroscience 84, 619–625.

N'Gouemo, P., Morad, M., 2003a. Ethanol withdrawal seizure susceptibility is associated with upregulation of L- and P-type Ca^{2+} channel currents in rat inferior colliculus neurons. Neuropharmacology 45, 429–437.

N'Gouemo, P., Morad, M., 2003b. Voltage-gated calcium channel in adult inferior colliculus neurons. Neuroscience 120, 815–826.
N'Gouemo, P., Rogawaski, M.A., 2006. Alcohol withdrawal seizures. In: Pitkänen, A., Schwartzkroin, P.A., Moshé, S.L. (Eds.), Models of Seizures and Epilepsy. Elsevier, Amsterdam, pp. 161–177.
N'Gouemo, P., Yasuda, R.P., Morad, M., Faingold, C.L., 2003. Audiogenic Seizure Alters the Expression of Calcium and Potassium Channel Protein in Inferior Colliculus Neurons of the Genetically Epilepsy-prone Rat (GEPR-3) Program No. 212.20. Abstract Viewer/Planner. Society for Neuroscience, New Orlean, LA. Online.
N'Gouemo, P., Morad, M., Faingold, C.L., 2004. Upregulation of Calcium Channel Current is Associated with Audiogenic Seizure Susceptibility in Inferior Colliculus Neurons of the Genetically Epilepsy-prone Rat (GEPR-3) Program No. 566.4. Abstract Viewer/Planner. Society for Neuroscience, San Diego, CA. Online.
N'Gouemo, P., Faingold, C.L., Morad, M., 2006a. Calcium-activated Potassium Currents are Downregulated in Rat Inferior Colliculus Neurons of the Genetically Epilepsy-prone Rat (GEPR-3). American Epilepsy Society. Abstract Viewer, Poster # 3.072.
N'Gouemo, P., Yasuda, R., Morad, M., 2006b. Ethanol withdrawal is accompanied by downregulation of calcium channel alpha 1B subunit in rat inferior colliculus neurons. Brain Research 1108, 216–220.
Neher, E., 1992. Correction for liquid junction potentials in patch clamp experiments. Methods in Enzymology 207, 123–131.
Raisinghani, M., Faingold, C.L., 2005a. Neurons in the amygdala play an important role in the neuronal network mediating a clonic form of audiogenic seizures both before and after audiogenic kindling. Brain Research 1032, 131–140.
Raisinghani, M., Faingold, C.L., 2005b. Evidence that the perirhinal cortex as a requisite component in the seizure network following seizure repetition in an inherited form of generalized clonic seizures. Brain Research 1048, 193–201.
Reigel, C.E., Daily, J.W., Jobe, P.C., 1986. The genetically epilepsy-prone rat: an overview of seizure-prone characteristics and responsiveness to anticonvulsant drugs. Life Science 39, 763–774.
Sanabria, E.R.G., Su, H., Yaari, Y., 2001. Initiation of network bursts by Ca^{2+}-dependent intrinsic bursting in rat pilocarpine model of temporal lobe epilepsy. Journal of Physiology 532, 205–226.
Stables, J.P., Bertram, E.H., White, H.S., Coulter, D.A., Dichter, M.A., Jacobs, M.P., Löscher, W., Lowenstein, D.H., Moshé, S.L., Noebels, J.L., Davis, M., 2002. Models of epilepsy and epileptogenesis: reports from the NIH workshop, Bethesda, Maryland. Epilepsia 43, 1410–1420.
Su, H., Sochivko, D., Becker, A., Chen, J., Jiang, Y., Yaari, Y., Beck, H., 2002. Upregulation of a T-type of Ca^{2+} channel causes a long-lasting modification of neuronal firing mode after status epilepticus. Journal of Neuroscience 22, 3645–3655.
Suzuki, T., Delgado-Escueta, A.V., Aguan, K., Alonso, M.E., Shi, J., Yuji, H., et al., 2004. Mutations in EFHC1 cause juvenile myoclonic epilepsy. Nature Genetics 36, 842–849.
Tsakiridou, E., Bertollini, L., De Curtis, M., Avanzini, G., Pape, H.C., 1995. Selective increase in T-type calcium conductance of reticular thalamus neurons in rat model of absence epilepsy. Journal of Neuroscience 15, 3110–3117.
Verma-Ahuja, S., Evans, M.S., Pencek, T.L., 1995. Evidence for decreased calcium dependent potassium conductance in hippocampal CA3 neurons of genetically epilepsy-prone rats. Epilepsy Research 22, 137–144.
Vreugdenhil, M., Wadman, W.J., 1992. Enhancement of calcium currents in hippocampal CA1 neurons induced kindling epileptogenesis. Neuroscience 49, 373–381.
Wang, S., Ding, M., Wu, D., ZhanChen, Z., 2007. ω-Conotoxin MVIIA inhibits amygdaloid kindled seizures in Sprague–Dawley rats. Neuroscience Letters 413, 163–167.
Weiergraber, M., Henry, M., Kreiger, A., Kamp, M., Radhakrishnan, K., Hescheler, H., Schneider, T., 2006. Altered seizure susceptibility in mice lacking the $Ca_v2.3$ E-type Ca^{2+} channel. Epilepsia 47, 839–850.
Weiergraber, M., Henry, M., Radhakrishnan, K., Hescheler, H., Schneider, T., 2007. Hippocampal seizure resistance and reduced neuronal excitotoxicity in mice lacking the CaV2.3 E/R-type voltage-gated calcium channel. Journal of Neurophysiology 97, 3660–3669.